Research Article Vol. 2, No. 3 / 15 March 2019 / OSA Continuum 938

Maximum amplification of a string transverse-force amplifier in fiber Bragg grating accelerometers

KUO LI,[1,2,*] TOMMY H. T. CHAN,[2] MAN HONG YAU,[2] DAVID P. THAMBIRATNAM,[2] AND HWA YAW TAM[3]

[1] School of Electronic and Electrical Engineering, Bengbu University, Bengbu 233030, China
[2] Civil Engineering and Built Environment, Queensland University of Technology, Brisbane 4000, Australia
[3] Photonic Research Centre, The Hong Kong Polytechnic University, Hong Kong SAR, China
[*] tolikuo@gmail.com

Abstract: Fiber Bragg grating (FBG) accelerometers using transverse forces are very sensitive. When a transverse force is applied to a lightly stretched string fixed by its two ends, a much stronger axial force along the string will be induced. So, the transverse force is amplified and converted into the axial force. At a given pre-strain of the string, the maximum amplification and requirements to obtain it have not been clearly demonstrated. Here, we theoretically prove and experimentally verify that the maximum amplification occurs when the strain induced by the transverse force approximately equals the pre-strain. This revelation improves the understanding of FBG accelerometers using transverse forces.

1. Introduction

FBG (fiber Bragg grating) has many inherent advantages such as frequency modulation and easy multiplexing. FBG is sensitive to its strain change, based on which many FBG accelerometers have been proposed [1–10]. The original FBG accelerometer was developed by embedding/attaching an FBG to a base and transferring the strain change of the base to the FBG [1,2]. But its sensitivity was usually low. To improve the sensitivity, an FBG was fixed by its two ends, and an inertial object was moved axially along the FBG [3–6]. To further improve the sensitivity while using the same inertial object, the inertial object was moved transversely to the FBG [8–11]. When a 1.76-gram inertial object was moved axially and transversely, its sensitivity in the transverse direction was 24 times that in the axial direction [10].

Figure 1 shows that a weightless string is lightly stretched and fixed by its two ends. Then, when a transverse force is applied to the middle, a much stronger axial force along the string can be induced. The transverse force is amplified and converted into the axial force. The amplification would be infinite if the pre-strain could be negligible and the transverse force could be infinitesimal. However, the pre-strain is often not negligible. (Strain is the ratio of the length change to the original length, and pre-strain is the strain when the string is fixed. As the transverse force increases, the string becomes longer and its strain increases.) 0.10 and 0.68N transverse forces were amplified 9.60 and 5.05 times at ~0.00004 pre-strain and 3.15 and 3.84 times at ~0.00155 pre-strain, respectively [11]. The amplification was different for different transverse forces or at different pre-strains.

How to obtain the maximum amplification at a given pre-strain? What is the maximum amplification? As far as we know, these problems have not been solved yet. We solve them in this paper. Firstly, at 3 different pre-strains, the relationships between the induced-strains and amplifications are simulated by 3 curves, respectively. There is a peak in every curve, which is the stationary point of the curve. Secondly, the horizontal and vertical coordinates of the peaks are located in the simulated results. The vertical coordinates are the maximum

#344463 https://doi.org/10.1364/OSAC.2.000938
Journal © 2019 Received 7 Sep 2018; revised 20 Dec 2018; accepted 4 Jan 2019; published 13 Mar 2019

OSA CONTINUUM

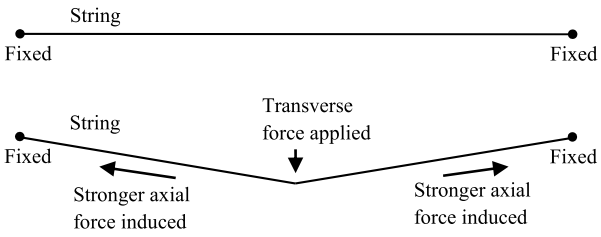

Fig. 1. Diagram of the string transverse-force amplifier

amplifications at the pre-strains. The horizontal coordinates, the induced-strains at the maximum amplifications, are the requirements to obtain the maximum amplifications. It is found that the induced-strains at the maximum amplifications approximately equal to the pre-strains. Thirdly, the simulated results are experimentally verified by using an FBG fixed by its two ends. The distance between the two ends was changed to apply a pre-strain. Then, different weights were hung in the middle. The pre-strains, induced-strains and axial forces were calculated based on the resonant-wavelength-change of the FBG. Lastly, theoretically, at any pre-strain, the induced-strain at the maximum amplification is found by using calculous to find the stationary point. The maximum amplification is found accordingly. The 3 pre-strains used in the simulations and experiments are substituted into the equations. The theoretical results are compared with the simulated results. The theoretical induced-strain at the maximum amplification is approximated to the pre-strain by using Maclaurin series. The simulated and experimental results and theoretical calculations are in Dataset 1 [12].

2. Simulation

When the applied position is at the middle of the string, the amplification is [11]:

$$\Delta F_l/F_t = \frac{\Delta\varepsilon(\Delta\varepsilon+1)}{2(\varepsilon+\Delta\varepsilon)\sqrt{2\Delta\varepsilon+\Delta\varepsilon^2}}, \tag{1}$$

where F_t, ΔF_l, ε, and $\Delta\varepsilon$ are the transverse force applied, induced-axial-force by F_t, pre-strain before F_t is applied, and induced-strain, respectively. The induced-strain ($\Delta\varepsilon$) is the change of the strain when the transverse force (F_t) is applied.

Table 1 shows the simulated relationships between the induced-stain and amplification at the 3 pre-strains based on Eq. (1). The induced-stain ($\Delta\varepsilon$) was increased from 0.0000001 to 0.01 in steps of 0.0000001. The amplifications ($\Delta F_l/F_t$) were calculated based on Eq. (1).

Table 1. Simulated relationships at the 3 pre-strains based on Eq. (1)

Induced-strain ($\Delta\varepsilon$)	Pre-strain 0.0000431	Pre-strain 0.0005177	Pre-strain 0.0015530
	Amplification ($\Delta F_l/F_t$)		
0.0000001	2.59	0.22	0.07
0.0000002	3.65	0.31	0.10
0.0000003	4.46	0.37	0.12
...	...	...	...
0.01	3.55	3.39	3.08

Figure 2 shows the simulated and experimental results. The first 3 graphs show the results separately, while the last graph shows them together. The 3 curves show the simulated relationships between the induced-strain ($\Delta\varepsilon$) and amplification ($\Delta F_l/F_t$) in Eq.(1) at the 3 pre-strains. Although

OSA CONTINUUM

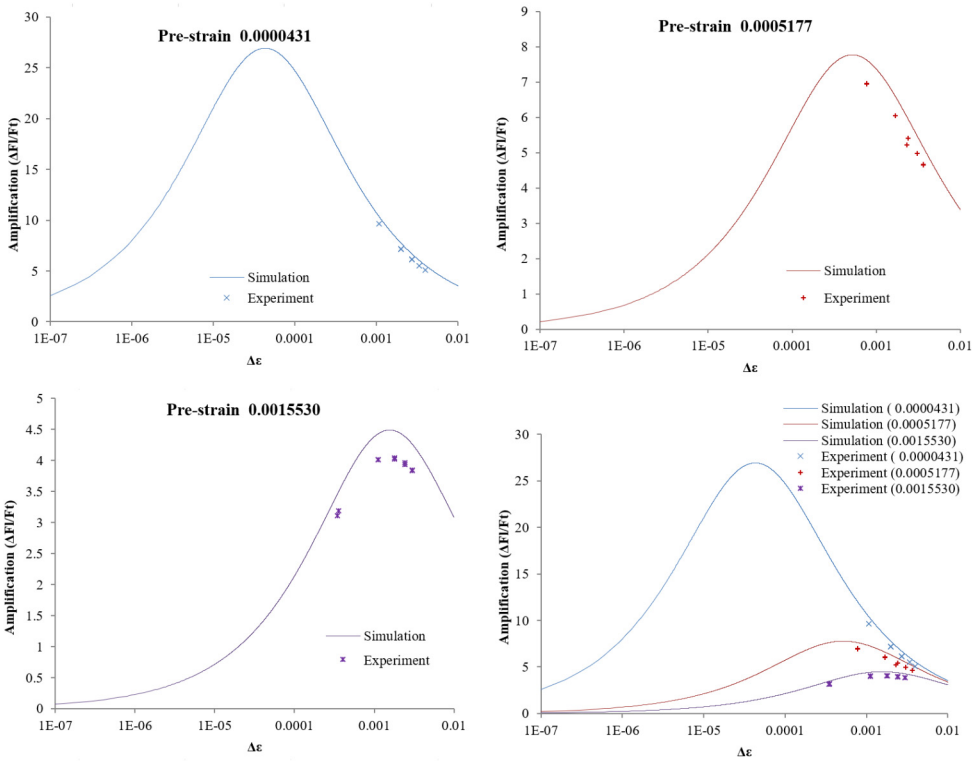

Fig. 2. Simulated and experimental results at the 3 different pre-strains

the 3 curves look similar, the smaller the pre-strain, the earlier the maximum amplification appears and larger the maximum amplification. At the beginnings, when the induced-strains increase, the amplifications increase; as the induced-strains keep increasing, the amplifications reach their maximums and then start to decrease. At the ends, the differences between the 3 curves become indistinct.

To locate the coordinates of the peaks in Fig. 2, Table 2 shows the extracted results from Table 1. The maximum amplifications and required induced-strains are highlighted by red colour. It shows that the induced-strains at the maximum amplifications approximately equal the corresponding pre-strains.

OSA CONTINUUM

Table 2. Maximum amplifications and the required induced-strains at the 3 pre-strains

Induced-strain ($\Delta\varepsilon$)	Pre-strain 0.0000431	Pre-strain 0.0005177	Pre-strain 0.0015530
		Amplification ($\Delta F_l/F_t$)	
0.0000001	2.58804183473	0.21592006037	0.07198725598
0.0000002	3.65159137934	0.30529814004	0.10179880680
...	...	...	...
0.0000429	26.92769468135		
0.0000430	26.92775135602		
0.0000431	26.92777153752		
0.0000432	26.92775547906		
0.0000433	26.92770343193		
...	...	...	...
0.0005183		7.77239073874	
0.0005184		7.77239085095	
0.0005185		7.77239089096	
0.0005186		7.77239085880	
0.0005187		7.77239075452	
...			
0.0015601			4.49102888837
0.0015602			4.49102889402
0.0015603			4.49102889508
0.0015604			4.49102889155
0.0015605			4.49102888343
...	...	...	...

3. Experiment

Figure 3 shows the experimental setups. The FBG was manufactured on bending insensitive fibers (Silibend G.657.B, Silitec Fibers Ltd.) by using phase masks, ~6 mm in length, ~0.2 nm of 3 dB bandwidth, and ~90% of reflectivity. The FBG was fixed between the two pillars, and away from the middle where the basket was hung. One of the pillars could be moved horizontally by turning the screw to stretch the FBG to apply a pre-strain. After the FBG was pre-strained, weights were placed on the FBG at the middle of the two pillars to apply the transverse forces. The distance between the pillars was ~100 mm. The free-state resonant wavelengths of the FBG used was ~1535.57 nm at room temperature.

In Fig. 2, the discrete marks were the experimental results, which follow the trends of the simulated curves. Experimentally, when the FBG was stretched, its resonant-wavelength-change divided by 1159.02 nm was its strain-change, and divided by 1.33 nm/N was its axial-force-change [11]. The 3 pre-strains (0.0000431, 0.0005177 and 0.0015530) correspond with the resonant-wavelength-changes 0.05, 0.6 and 1.8 nm, respectively.

Table 3 shows the experimental results at the pre-strain 0.0000431. The screw in Fig. 3(a) was tuned to stretch the FBG, and made its resonant wavelength increase ~0.05 nm to apply the pre-strain 0.0000431. Then, a transverse force was applied by hanging a weight at the middle, and its induced-resonant-wavelength-change was recorded. Then, (a) the transverse force was found by converting mass into weight, (b) the induced-strain $\Delta\varepsilon$ was calculated by dividing the induced-resonant-wavelength-changes by 1159.02 nm, and (c) the amplification $\Delta F_l/F_t$ was calculated by firstly dividing the induced-resonant-wavelength-change by 1.33 nm/N to get the

OSA CONTINUUM

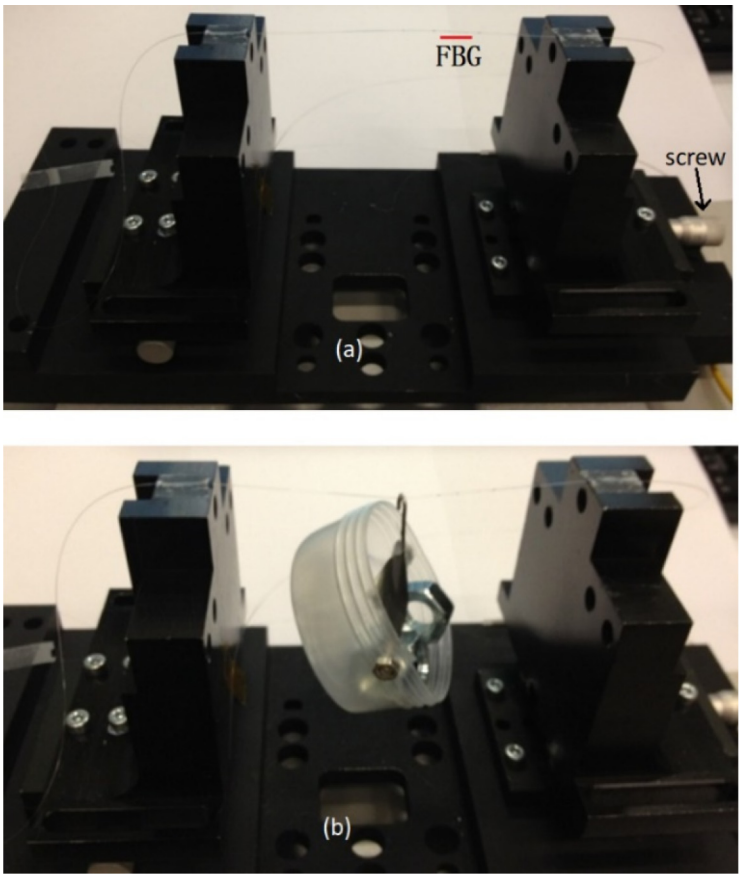

Fig. 3. Experimental setups: applying a pre-strain (a) and transverse force (b)

induced-axial-force and then dividing the induced-axial-force by the transverse force. It was repeated again.

Table 3. Experimental results at the pre-strain 0.0000431

Weight hung [gram]	transverse force [N]	Induced-wavelength-change [nm]	$\Delta\varepsilon$	$\Delta F_l/F_t$
9.89	0.097	1.245	0.00107	9.66
24.74	0.242	2.319	0.00200	7.19
39.5	0.387	3.167	0.00273	6.15
54.41	0.533	3.919	0.00338	5.53
69.45	0.681	4.607	0.00397	5.09
9.89	0.097	1.242	0.00107	9.63
24.74	0.242	2.308	0.00199	7.16
39.5	0.387	3.157	0.00272	6.13
54.41	0.533	3.902	0.00337	5.50
69.45	0.681	4.588	0.00396	5.07

OSA CONTINUUM

4. Theory

To find the stationary point of Eq. (1), its derivative is found and equalled to zero:

$$\begin{aligned}\frac{d(\Delta F_l/F_t)}{d\Delta\varepsilon} &= \frac{d\left(\frac{\Delta\varepsilon(\Delta\varepsilon+1)}{2(\varepsilon+\Delta\varepsilon)\sqrt{2\Delta\varepsilon+\Delta\varepsilon^2}}\right)}{d\Delta\varepsilon}\\ &= \frac{1}{2}\frac{(2\Delta\varepsilon+1)\left[(\varepsilon+\Delta\varepsilon)\sqrt{2\Delta\varepsilon+\Delta\varepsilon^2}\right]-\Delta\varepsilon(\Delta\varepsilon+1)(2\Delta\varepsilon+\Delta\varepsilon^2)^{-\frac{1}{2}}(\varepsilon+\varepsilon\Delta\varepsilon+3\Delta\varepsilon+2\Delta\varepsilon^2)}{\left[(\varepsilon+\Delta\varepsilon)\sqrt{2\Delta\varepsilon+\Delta\varepsilon^2}\right]^2}\\ &= 0\end{aligned}$$

So,

$$\begin{aligned}(2\Delta\varepsilon+1)\left[(\varepsilon+\Delta\varepsilon)\sqrt{2\Delta\varepsilon+\Delta\varepsilon^2}\right]-\Delta\varepsilon(\Delta\varepsilon+1)(2\Delta\varepsilon+\Delta\varepsilon^2)^{-\frac{1}{2}}(\varepsilon+\varepsilon\Delta\varepsilon+3\Delta\varepsilon+2\Delta\varepsilon^2)&=0\\ (2\Delta\varepsilon+1)(\varepsilon+\Delta\varepsilon)(2\Delta\varepsilon+\Delta\varepsilon^2)-\Delta\varepsilon(\Delta\varepsilon+1)(\varepsilon+\varepsilon\Delta\varepsilon+3\Delta\varepsilon+2\Delta\varepsilon^2)&=0\\ (2\Delta\varepsilon+1)(\varepsilon+\Delta\varepsilon)(2+\Delta\varepsilon)-(\Delta\varepsilon+1)(\varepsilon+\varepsilon\Delta\varepsilon+3\Delta\varepsilon+2\Delta\varepsilon^2)&=0\\ \varepsilon\Delta\varepsilon^2+(3\varepsilon-1)\Delta\varepsilon+\varepsilon&=0.\end{aligned} \tag{2}$$

To solve the above quadratic equation, we get:

$$\Delta\varepsilon=\frac{1-3\varepsilon-\sqrt{1-6\varepsilon+5\varepsilon^2}}{2\varepsilon}. \tag{3}$$

The other solution of Eq.(2), $\Delta\varepsilon=\left(1-3\varepsilon+\sqrt{1-6\varepsilon+5\varepsilon^2}\right)/(2\varepsilon)$, is abandoned, because (a) as $0<\varepsilon\ll 1$, $\Delta\varepsilon$ is much larger than 1 and (b) $\Delta\varepsilon$ being much larger than 1 is practically impossible.

By substituting Eq.(3) into Eq.(1), the maximum amplification is:

$$\begin{aligned}\Delta F_l/F_t &= \frac{\Delta\varepsilon(\Delta\varepsilon+1)}{2(\varepsilon+\Delta\varepsilon)\sqrt{2\Delta\varepsilon+\Delta\varepsilon^2}}\\ &= \frac{\Delta\varepsilon+1}{2(\varepsilon+\Delta\varepsilon)\sqrt{\frac{2}{\Delta\varepsilon}+1}}\\ &= \frac{\frac{1-3\varepsilon-\sqrt{1-6\varepsilon+5\varepsilon^2}}{2\varepsilon}+1}{2\left(\varepsilon+\frac{1-3\varepsilon-\sqrt{1-6\varepsilon+5\varepsilon^2}}{2\varepsilon}\right)\sqrt{\frac{4\varepsilon}{1-3\varepsilon-\sqrt{1-6\varepsilon+5\varepsilon^2}}+1}}\end{aligned} \tag{4}$$

Table 4 shows the comparison between the simulated and the theoretical results at the 3 pre-strains. The induced-strains at the maximum amplifications located in the simulated results shown in the Table 2 are compared with the theoretical ones obtained by substituting the 3 pre-strains into the Eq. (3). The maximum amplifications located in the simulated results shown in the Table 2 are compared with the theoretical ones obtained by Eq. (4). The simulated and the theoretical results

Table 4. Comparison between the simulated and the theoretical results

Pre-strain	Induced-strain at the maximum amplification		Maximum amplification	
	by simulation	by Eq. (3)	by simulation	by Eq. (4)
0.0000431	0.0000431	0.000043106	26.92777153752	26.92777159380
0.0005177	0.0005185	0.000518505	7.77239089096	7.77239089107
0.001553	0.0015603	0.001560273	4.49102889508	4.49102889525

OSA CONTINUUM

agree with each other exactly, although there are differences between them. Their differences are due to the steps of the simulation 0.0000001. The maximum amplifications by Eq.(4) are always slightly larger than the simulation ones. Their differences will keep reducing, if the steps of the simulation keep decreasing.

As $0<\varepsilon \ll 1$, by using Maclaurin series ($\sqrt{1+x} = 1 + \frac{1}{2}x - \frac{1}{8}x^2 + \circ(x)$), Eq. (3) can be simplified as

$$\begin{aligned}
\Delta\varepsilon &= \frac{1-3\varepsilon-\left(1+\frac{1}{2}(5\varepsilon^2-6\varepsilon)-\frac{1}{8}(5\varepsilon^2-6\varepsilon)^2+\circ(5\varepsilon^2-6\varepsilon)\right)}{2\varepsilon} \\
&= \frac{1-3\varepsilon-\left(1+\frac{5\varepsilon^2}{2}-3\varepsilon-\frac{36\varepsilon^2}{8}+\circ(\varepsilon)\right)}{2\varepsilon} \\
&= \frac{1-3\varepsilon-(1-3\varepsilon-2\varepsilon^2+\circ(\varepsilon))}{2\varepsilon} \\
&\approx \frac{1-3\varepsilon-(1-3\varepsilon-2\varepsilon^2)}{2\varepsilon} \\
&= \varepsilon.
\end{aligned} \tag{5}$$

Therefore, the maximum amplification is approximately:

$$\begin{aligned}
\Delta F_l/F_t &= \frac{\Delta\varepsilon(\Delta\varepsilon+1)}{2(\varepsilon+\Delta\varepsilon)\sqrt{2\Delta\varepsilon+\Delta\varepsilon^2}} \\
&\approx \frac{\varepsilon(\varepsilon+1)}{4\varepsilon\sqrt{2\varepsilon+\varepsilon^2}} \\
&= \frac{(\varepsilon+1)}{4\sqrt{2\varepsilon+\varepsilon^2}} \\
&\approx \frac{1}{4\sqrt{2\varepsilon}} \\
&= \frac{1}{8}\sqrt{\frac{2}{\varepsilon}}\,.
\end{aligned} \tag{6}$$

5. Conclusion

The fact shown in Fig. 2 that the marks obtained from the experiments follow the simulated curves verifies the simulation. The fact shown in Table 4 that the simulated values at the maximum amplifications agree exactly with the theoretical ones verifies the theoretical analysis. At a given pre-strain, the maximum amplification is shown in Eq. (4) and Eq. (6), and occurs when the induced-strain approximately equals the pre-strain as shown in Eq. (3) and Eq. (5).

This finding can be used in the FBG accelerometers using transverse forces. The pre-strain changes due to the slack of the epoxy glue used to fix the two ends of the FBG or the temperature-induced distance-change between the two fixed ends. To ensure that the FBG is always pre-strained, a moderate pre-strain may be applied. For example, assume that 0.0005177 pre-strain (0.6 nm pre-stretch) is applied. The maximum amplification is about 7.77 according to Eq. (6), $\frac{1}{8}\sqrt{\frac{2}{0.0005177}} \approx 7.77$, and occurs when the induced-wavelength-change is about 0.6 nm. It corresponds with 0.45N ($\frac{0.6\text{nm}}{1.33\text{nm/N}} = 0.45\text{N}$) axial force [11]. The transverse force being amplified most is 0.058N (0.45N/7.77 = 0.058N). The inertial object weighted 5.92gram ($\frac{0.058\text{N}}{0.0098\text{N/gram}} = 5.92\text{gram}$) works most efficiently.

OSA CONTINUUM

Funding

Queensland University of Technology (QUT); Research Grants Council of the Hong Kong SAR (RGC Ref No. 512006); Bengbu University, China (BBXY2018KYQD02).

Acknowledgments

This research is supported by the doctorate scholarships provided by Queensland University of Technology, Research Grants Council of the Hong Kong SAR (RGC Ref No. 512006), and the start-up research fund from Bengbu University (BBXY2018KYQD02).

References

1. T. A. Berkoff and A. D. Kersey, "Experimental demonstration of a fiber Bragg grating accelerometer," IEEE Photonics Technol. Lett. **8**(12), 1677–1679 (1996).
2. M. D. Todd, G. A. Johnson, B. A. Althouse, and S. T. Vohra, "Flexural beam-based fiber Bragg grating accelerometers," IEEE Photonics Technol. Lett. **10**(11), 1605–1607 (1998).
3. A. Stefani, S. Andresen, W. Yuan, N. Herholdt-Rasmussen, and O. Bang, "High Sensitivity Polymer Optical Fiber-Bragg-Grating-Based Accelerometer," IEEE Photonics Technol. Lett. **24**(9), 763–765 (2012).
4. P. F. Costa Antunes, C. A. Marques, H. Varum, and P. S. Andre, "Biaxial optical accelerometer and high-angle inclinometer with temperature and cross-axis insensitivity," IEEE Sens. J. **12**(7), 2399–2406 (2012).
5. Y. X. Guo, D. S. Zhang, Z. D. Zhou, L. Xiong, and X. W. Deng, "Welding-packaged accelerometer based on metal-coated FBG," Chin. Opt. Lett. **11**(7), 21–23 (2013).
6. Y. Zhang, W. Zhang, Y. Zhang, L. Chen, T. Yan, S. Wang, L. Yu, and Y. Li, "2-d medium–high frequency fiber bragg gratings accelerometer," IEEE Sens. J. **17**(3), 614–618 (2017).
7. N. Basumallick, P. Biswas, R. Chakraborty, S. Chakraborty, K. Dasgupta, and S. Bandyopadhyay, "Fibre bragg grating based accelerometer with extended bandwidth," Measurement Science & Technology **27**(3), 035008 (2016).
8. K. Li, T. H. T. Chan, M. H. Yau, T. Nguyen, D. P. Thambiratnam, and H. Y. Tam, "Very sensitive fiber Bragg grating accelerometer using transverse forces with an easy over-range protection and low cross axial sensitivity," Appl. Opt. **52**(25), 6401–6410 (2013).
9. K. Li, T. H. T. Chan, M. H. Yau, D. P. Thambiratnam, and H. Y. Tam, "Experimental verification of the modified spring-mass theory of fiber Bragg grating accelerometers using transverse forces," Appl. Opt. **53**(6), 1200–1211 (2014).
10. K. Li, T. H. T. Chan, M. H. Yau, D. Thambiratnam, and H. Y. Tam, "Biaxial fiber Bragg grating accelerometer using axial and transverse forces," IEEE Photonics Technol. Lett. **26**(15), 1549–1552 (2014).
11. K. Li, M. H. Yau, T. H. T. Chan, D. Thambiratnam, and H. Y. Tam, "Fiber Bragg grating strain modulation based on nonlinear string transverse-force amplifier," Opt. Lett. **38**(3), 311–313 (2013).
12. K. Li and M. H. Yau, "Maximum amplification of string transverse-force amplifier (simulated, experimental and theoretical results)," figshare (2018), https://doi.org/10.6084/m9.figshare.7054373.